Polymer 53 (2012) 1277–1281

Contents lists available at SciVerse ScienceDirect

Polymer

journal homepage: www.elsevier.com/locate/polymer

Effect of crystal structure on polarization reversal and energy storage of ferroelectric poly(vinylidene fluoride-*co*-chlorotrifluoroethylene) thin films

Ruixuan Han [a,b], Jiezhu Jin [a], Paisan Khanchaitit [a], Jingkang Wang [b], Qing Wang [a,*]

[a] Department of Materials Science and Engineering, The Pennsylvania State University, University Park, PA 16802, USA
[b] School of Chemical Engineering and Technology, Tianjin University, Tianjin 300072, China

ARTICLE INFO

Article history:
Received 15 November 2011
Received in revised form
2 February 2012
Accepted 3 February 2012
Available online 8 February 2012

Keywords:
Ferroelectric polymers
Polarization
Dielectric properties

ABSTRACT

A series of ferroelectric poly(vinylidene fluoride-*co*-chlorotrifluoroethylene) films with different crystallite sizes have been obtained by varying the film processing conditions. The impact of the crystallite size on the dipole switching and the electric energy density has been systematically studied by the electric displacement–electric field hysteresis loop measurements. The films with smaller crystallite sizes display larger polarizability, as evidenced by higher maximum polarization and lower dipole switching field in the charging process. Small crystals also facilitate fast dipole depolarization during the discharging process. Consequently, superior released energy densities have been achieved in the films containing small sizes of the ferroelectric crystallite domains. On the other hand, large crystallite sizes are beneficial for the dielectric breakdown strength and the Weibull distribution of the breakdown field of the films. This study sheds new fundamental light on the optimization of the crystal structures of the ferroelectric polymers for high electric energy storage applications.

1. Introduction

The development of new materials with high energy density is viewed as a critical enabling step for the realization of compact, low-cost and high-performance energy storage devices for applications in portable electronics, electric power systems and next-generation vehicles [1,2]. Extensive studies have been carried out on polymeric materials for film capacitors, owing to their great processability, high breakdown strength, and self-healing mechanism [3,4]. Ferroelectric polymers represented by poly(vinylidene fluoride) (PVDF) and its copolymers are emerging as the promising benchmark candidates for this class of materials [5–7]. The presence of strong polarization from C–F bonds and the spontaneous orientation of dipoles in the crystalline phases give rise to high dielectric responses in PVDF. By modifying PVDF with chlorotrifluoroethylene (CTFE) or hexafluoropropylene (HFP), the resulting P(VDF-CTFE) and P(VDF-HFP) copolymers exhibit capacitive energy densities of ~17 J/cm^3 with millisecond discharge rates [8], which are substantially higher than the current state-of-the-art polymer capacitors, biaxially stretched polypropylene (BOPP) with an energy density of ~3 J/cm^3 [9].

The molecular origin of these properties, however, has not been well understood. It is recognized that the electrostatic energy storage capacity of the ferroelectric polymers critically depends on their polarization switching ability under the applied electric field, which in turn is closely related to the crystalline structures and morphologies [10–15]. PVDF with different chain conformations can be packed into various crystal lattices to form a range of crystalline phases such as the non-polar α phase and polar β, δ and γ phases depending on the processing conditions [5,6]. The existence of bulky CTFE and HFP in the copolymers stabilizes the *trans-gauche* (TGTG′) chain conformation and the non-polar α phase, which facilitates the phase transformation under an applied field and avoids early polarization saturation [16]. The P(VDF-CTFE) and P(VDF-HFP) copolymers therefore display narrower polarization hysteresis loops and broadened relaxation process, and consequently, higher discharged energy densities than those of normal ferroelectrics [8]. More recently, the effect of the crystal orientation on the stored/discharged energy densities of P(VDF-HFP) has been examined [15]. It is observed that the transverse crystals with *c*-axes oriented perpendicular to the applied field are desired for larger polarizability and higher electric energy storage as compared to those in the crystal with the *c*-axes aligned parallel to the field.

It is the focus of this work to better understand the dipole reorientation and switching mechanisms of ferroelectric polymers in response to the applied electric field and elucidate their relationship with the electric energy storage properties. A variety of

* Corresponding author.
E-mail address: wang@matse.psu.edu (Q. Wang).

0032-3861/$ – see front matter © 2012 Elsevier Ltd. All rights reserved.
doi:10.1016/j.polymer.2012.02.004

crystalline sizes were obtained in P(VDF-CTFE) thin films by systematically varying the film fabrication and processing conditions. The dielectric properties of P(VDF-CTFE) at high electric fields were studied by using electric displacement–electric field (D–E) hysteresis loops and their derivative curves. It is conclusively demonstrated that the films with small crystals have low critical fields of ferroelectric switching and high released energy densities, whereas large crystals are beneficial for the dielectric breakdown strength and the Weibull distribution of the breakdown field of the films.

2. Experimental section

2.1. Materials and preparation of P(VDF-CTFE) films

P(VDF-CTFE) with 15 wt% CTFE was purchased from Solvay Solex Co. Film **I** was prepared by hot-pressing the resin at 230 °C followed by immediately quenching in liquid nitrogen and then annealing at room temperature for 24 h. Film **II** was prepared in the same process as film **I**, but it was annealed at 70 °C for 48 h. Film **III** was prepared by hot-pressing the powder at 230 °C followed by cooling naturally to room temperature and then annealing at 110 °C for 24 h. Film **IV** was prepared in the same process as film **III**, but it was annealed at 110 °C for 48 h. Film **V** was prepared by hot-pressing the powder at 230 °C followed by annealing at 110 °C for 64 h. The thickness of the films was around 15–25 μm.

2.2. Characterization

The X-ray diffraction experiments were performed on a Philips MPD theta-2-theta powder Diffractometer. The X-ray wavelength is Cu $K_\alpha = 0.1542$ nm. The apparent crystallite sizes along $[020]_\alpha$ were calculated according to the Scherrer equation:

$$D_{hkl} = (K\cdot\lambda)/(\beta_{hkl}\cdot\cos\theta) \quad (1)$$

where D_{hkl} is the mean crystallite size along the [hkl] direction, K is the shape factor (a value of 0.94 is used in this case), λ is the wavelength, and β_{hkl} is the full width at half-maximum for the (hkl) diffraction. Fourier transform infrared (FTIR) spectra were obtained on a Niclotet Magna 560 FTIR spectrometer. Differential scanning calorimetry (DSC) was performed on a TA DSC Q-100 with a scanning rate of 10 °C /min. The degree of crystallinity was evaluated by:

$$\chi_c = H_f/\left(H_f^0\cdot\omega\right) \quad (2)$$

where $H_f^0 = 104.7$ J/g is the enthalpy of 100% crystalline PVDF. $\omega = 0.85$ is the weight percent of the PVDF in the copolymer. For the electrical measurements, gold electrodes with a thickness of 40 nm were sputtered on both surfaces of the polymer film. The D–E loops were measured by a modified Sawyer-Tower circuit and a linear variable differential transducer (LVDT), driven by a lock-in amplifier (Stanford Research Systems, model SR830). Electric fields ranging from 50 to 500 MV/m were applied across the polymer film using an amplified ramp waveform at 10 Hz. The breakdown field measurements were carried out using an electrostatic pull-down method, where a voltage ramp rate of 500 V/s was applied between a rounded electrode and the gold-coated polymer film.[17]

3. Results and discussion

P(VDF-CTFE) with less than 17 mol% CTFE content normally adopts the non-polar α phases. It is reported the thermal annealing leads to the formation of polar β- or γ-crystals in PVDF- and PVDF-based copolymers when the annealing temperature is below 50 °C [18]. To avoid interference from different crystal forms, the films were annealed above 70 °C. As expected, the α-crystals exclusively dominate in all of the films, as evidenced by the XRD profiles shown in Fig. 1, where only $(100)_\alpha$, $(020)_\alpha$, $(110)_\alpha$ and $(021)_\alpha$ reflections are observed at 2θ angles of 17.7, 18.4, 20.1, and 26.5°, respectively. This is further confirmed by the appearance of typical α-form absorption bands at 614, 532, 486, and 410 nm^{-1} in the FTIR spectra. As summarized in Table 1, the melting temperatures of the films remain unchanged at around 166–167 °C, whereas the size of the crystals decreases with the increase of the cooling rate. Films **I** and **II** were rapidly quenched in liquid nitrogen (i.e. −196 °C) from the melt state and have the smallest crystallite grain sizes of 21 and 25 nm, respectively. Films **V** and **IV** have the largest sizes of the crystals, i.e. 36 and 43 nm, respectively, as a result of the slowest cooling rate and subsequent annealing for long time at high temperatures.

The high-field dielectric properties of the P(VDF-CTFE) films were evaluated by the D–E hysteresis loop measurements. Note that the electric displacement primarily accounts for the amplitude of the dipole orientation (i.e. polarization) and the dielectric constant reveals the motion of the dipole orientation. Thus the derivative curves of the D–E loops, $(\partial D/\partial E)/\varepsilon_0$, are utilized to examine the dipole orientation dynamics of ferroelectric P(VDF-CTFE) films as a function of the electric field, where D represents the electric displacement, E is the applied field and ε_0 is the vacuum permittivity ($=8.85\times10^{-12}$ F/m) [13]. Fig. 2a and b exemplifies the D–E loops and $(\partial D/\partial E)/\varepsilon_0$ of the films **I** and **IV** at various electric fields. In the charging process, $(\partial D/\partial E)/\varepsilon_0$ shows a peak at a certain field upon the poling. At this peak electric field, the switching (or poling) rate of the dipoles reaches the maximum. The magnitude of this peak field indicates how easy the dipoles could be aligned by the electric field; the lower the peak field, the easier the dipoles could be oriented. For example, the fastest polarization reversal in film **I** occurs at an electric field of ~180 MV/m after the poling field reaches ≥250 MV/m, while the dipole switching field appears at ~290 MV/m for film **IV**. High orientation polarizability of film **I** is also demonstrated by the presence of larger maximum values of $(\partial D/\partial E)/\varepsilon_0$ and D. The maximum values of $(\partial D/\partial E)/\varepsilon_0$ are 19.2 and 16.6, and D are 0.064 and 0.046 at an electric field of 350 MV/m for films **I** and **IV**, respectively. The peak fields and maximum values of $(\partial D/\partial E)/\varepsilon_0$ of films **I**–**V** are summarized in Fig. 2c. The peak electric field increases steadily from 180 to 320 MV/m, which is

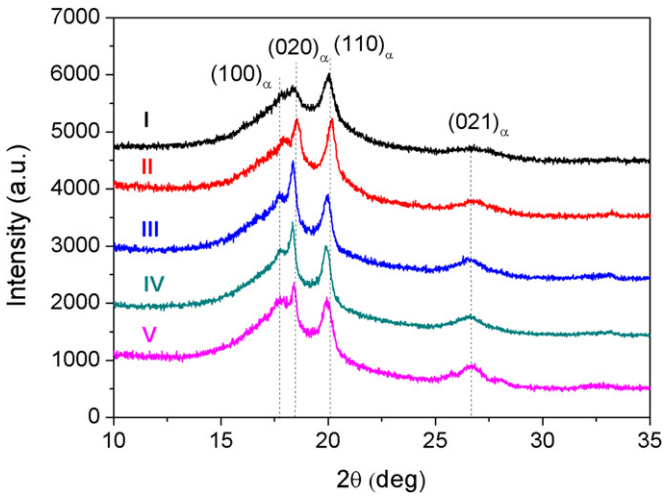

Fig. 1. Comparison of wide-angle X-ray diffraction patterns for films **I**-**V**.

Table 1
The processing conditions and crystalline structures of films **I**–**V**.

Films	Cooling conditions	Annealing temperature [°C]	Annealing time[h]	Heat of fusion [J/g]	Crystallinity [%]	Crystallite size [nm]
I	Quenching in liquid N_2	25	24	28.4	33	21
II	Quenching in liquid N_2	70	48	40.7	46	25
III	Cooling naturally to r.t	110	24	35.5	39	29
IV	Cooling naturally to r.t	110	48	30.5	34	36
V	Cooling to 110 °C	110	64	31.3	35	43

accompanied by the decrease of the maximum value of $(\partial D/\partial E)/\varepsilon_0$ from 19.3 to 13 with increasing the crystallite size from films **I** to **V**. This is a strong indication that the films containing small crystals are readily poled by the electric field, and have low switching fields and high poling rates in the charging process [19]. The relatively higher value of $(\partial D/\partial E)/\varepsilon_0$ shown in film **II** is likely due to its relatively higher crystallinity (i.e. 46%) in comparison to other films. Typical β-form absorption bands were found at 510, 471 and 443 cm^{-1} in the poled films, indicating the transformation from non-polar to polar phases induced by the applied field.

In the discharging process, the value of $(\partial D/\partial E)/\varepsilon_0$ increases with the decrease of the electric field and reaches the maximum at zero electric field. As presented in Fig. 2a and b, the maximum values of $(\partial D/\partial E)/\varepsilon_0$ are 26 and 15 for films **I** and **IV**, respectively, at a charging field of 300 MV/m. Fig. 2d plots the maximum value of $(\partial D/\partial E)/\varepsilon_0$ as a function of the poling field in the discharging process. Obviously, the maximum value of $(\partial D/\partial E)/\varepsilon_0$ intimately depends on the prior poling process and increases with the increase of the charging field. Moreover, it can be clearly seen that the maximum value of $(\partial D/\partial E)/\varepsilon_0$ decreases gradually in an order of films **I** > **II** > **III** > **IV** > **V**, which coincides with the increase of crystallite sizes. The obtained high maximum values of $(\partial D/\partial E)/\varepsilon_0$ imply that the small PVDF crystals are also easier to be depolarized in the discharging process, a trend similar to what is observed in the charging process.

It is generally believed that ferroelectric polarization reversal is accomplished by the nucleation of antiparallel domains, which

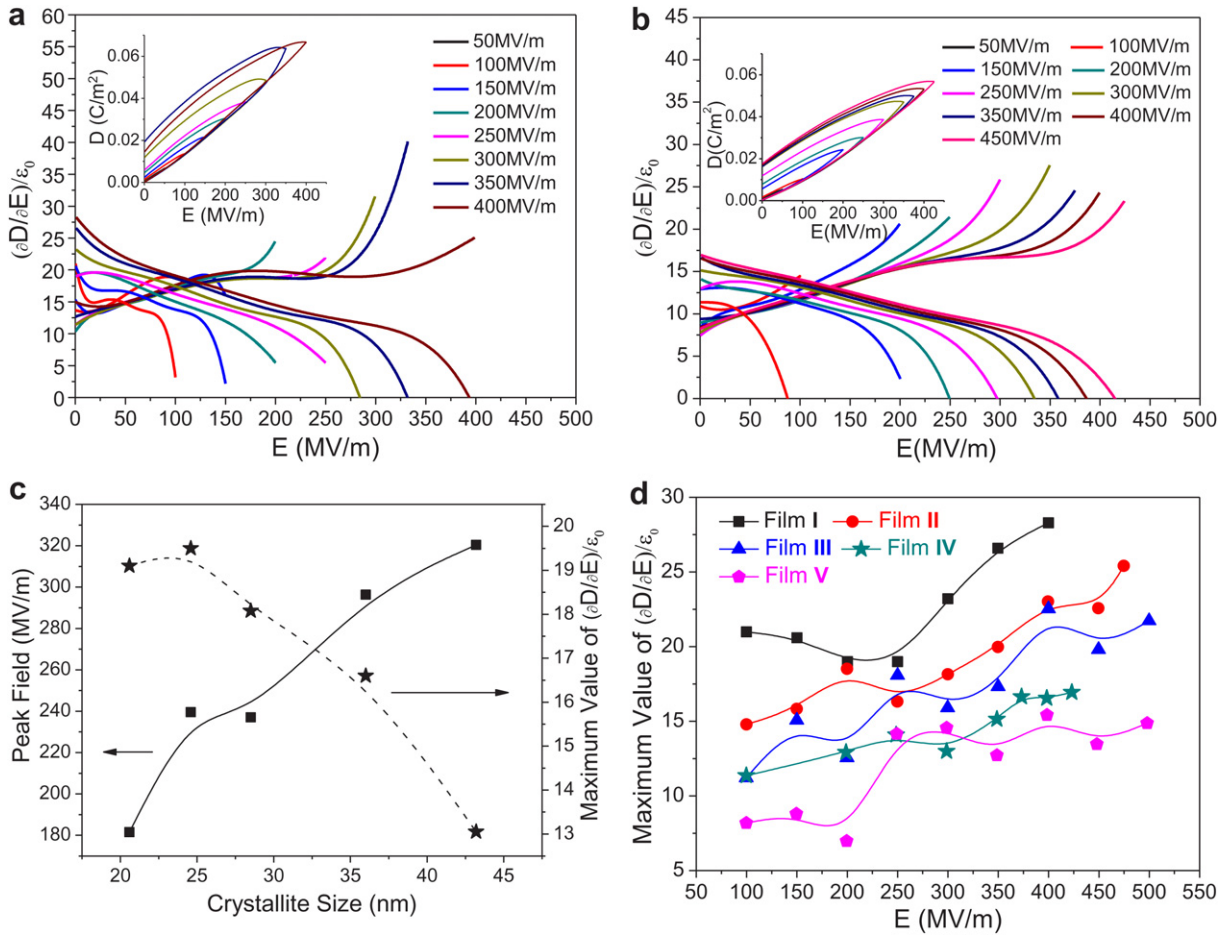

Fig. 2. $(\partial D/\partial E)/\varepsilon_0$ as a function of the electric field for (a) film **I** and (b) film **IV**. The inset shows the corresponding unipolar *D*–*E* hysteresis loops. (c) Dependence of the peak fields and the maximum values of $(\partial D/\partial E)/\varepsilon_0$ on the crystallite size in the charging process. (d) The maximum values of $(\partial D/\partial E)/\varepsilon_0$ of films **I**–**V** as a function of the poling field in the discharging process. The lines in (c) and (d) are guides for the eye.

normally takes place at the interface and/or the defect sites [20,21]. For the films dominated with non-polar α phase, the β phase nucleation shall be the control step of the phase transition in the charging process. The existence of more interfaces in the films with smaller crystals could offer more nucleation sites for the β phase and in turn decrease the energy barrier of the phase transition. Accordingly, the dipole reversal occurs at lower field in comparison to the films with larger crystallite sizes when the degrees of crystallinity of the films are similar. In the discharging process, small crystals create stronger depolarization field and introduce the larger depolarization force because of the existence of more crystal–amorphous interfacial areas and their higher polarization than those of the film containing large crystals at a given poling field. Therefore, the films with small crystals exhibit higher $(\partial D/\partial E)/\varepsilon_0$ values in the discharging process. On the other hand, large crystals facilitate the coupling interactions among the ferroelectric domains [14], and thus the dipole reversal becomes difficult, resulting in a high switching field and low rates of polarization and depolarization.

The ability of dipole reorientation in the P(VDF-CTFE) thin films has also been confirmed in the dependence of the maximum polarization on the electric field shown in Fig. 3a. There is a systematic dependence of the maximum polarization on the crystallite size, with film **I** exhibiting the highest polarization, and film **V** showing the lowest at any field. This result again suggests that the small size of the PVDF crystals is easily polarized. Additionally, under high fields (>350 MV/m), an inflection point of the maximum polarization appears in the films with small crystals, signifying that the polarization begins to saturate to complete the ferroelectric switching. The field of polarization saturation decreases systematically with the decrease of crystallite sizes from films **III** to **II** to **I**. On the contrary, no polarization saturation has been observed in films **IV** and **V** even at the applied field above 450 MV/m. As illustrated in Fig. 3b, consistent with the polarization results, the discharged electric energy density increases progressively with the decrease of the crystallite size from films **V** to **I**. In the charging process, the phase transition of α to β phases determines the electric energy stored in the film, while the relaxation from β to α phases during the discharging process is the main contribution to the electric energy released from the films. It can be rationalized that the films with smaller crystals contain more contents of the β phase after the charging process as evidenced by their high maximum polarization (see Fig. 2). Furthermore, high depolarization rates and low switching fields have been observed in the films with small crystals, implying that more β crystals could reverse in the discharging step and thereby yields higher released energy densities.

Breakdown strength is another key parameter in determining the energy storage capacity of the dielectric materials as the energy density is generally proportional to the square of the applied electric field. The electrical breakdown results were analyzed by a two-parameter Weibull distribution function:

$$P(E) = 1 - \exp\left[-(E/\alpha)^{\beta}\right] \quad (3)$$

where $P(E)$ is cumulative probability of electrical failure occurring at the electric field lower or equal to E, α is the characteristic breakdown strength which corresponds to a ~63.2% probability of failure, and β is the slope parameter that evaluates the scatter of data [17]. Fig. 4 presents the breakdown strengths of films **I** and **V**, where film **V** exhibits a slight improvement in the characteristic breakdown strength as compared to film **I** with smaller crystals. It is very noteworthy that film **V** has a β value of 13.1, which is two times that of film **I**; this denotes much uniform distribution of the breakdown strengths in film **V**. The breakdown distribution has an important implication for the reliability and the lifetime of energy storage devices.

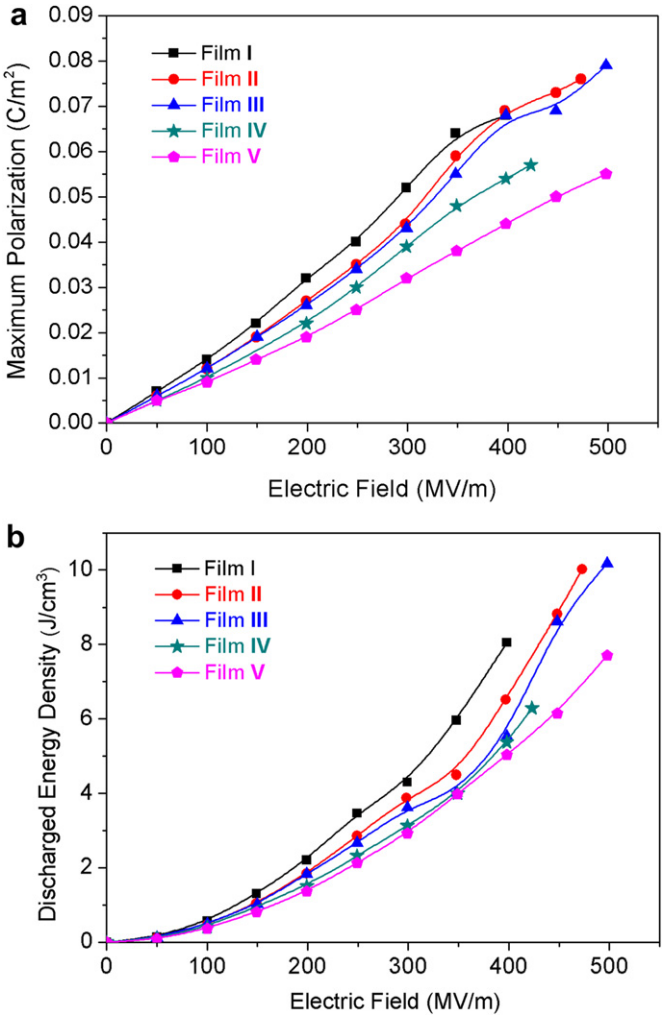

Fig. 3. (a) The maximum polarization and (b) discharged energy densities of films **I**–**V** at various electric fields.

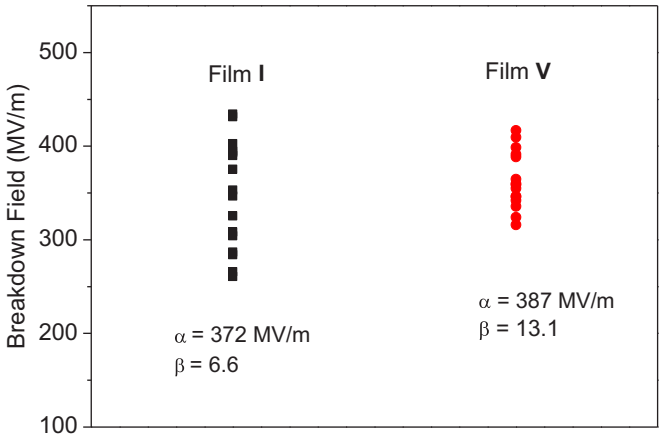

Fig. 4. Comparison of the strength and Weibull distribution of dielectric breakdown of films **I** and **V**.

4. Conclusions

In summary, we have investigated the dynamics of the polarization reversal in ferroelectric P(VDF-CTFE) films using derivative curves of the *D*–*E* loops. The dipole orientation characteristics of the ferroelectric polymers are found to be significantly affected by the crystallite size. The observed superior discharged energy densities in P(VDF-CTFE) with small crystals are a direct consequence of great reversibility of dipoles under the electric field as indicated by the presence of low dipole switching fields and high maximum polarization in the charging process and fast dipole depolarization in the discharging process. This effect of the crystallite structure on the dipole orientation behavior can play a vital role in determining and improving the high-field dielectric performance of the ferroelectric polymers for energy storage applications.

Acknowledgement

This work was supported by the National Science Foundation. RH acknowledges the graduate fellowship provided by the China Scholarship Council (CSC).

References

[1] Basic research needs for electrical energy storage. Washington, DC: Office of Basic Energy Science, US Department of Energy; 2007.
[2] Whittingham MS. MRS Bull 2008;33:411.
[3] Cao Y, Irwin PC, Younsi K. IEEE Trans Dielect Elect Insul 2004;11:797.
[4] Wang Q, Zhu L. J Polym Sci B Polym Phys 2011;49:1421.
[5] Lovinger A. Science 1983;220:1115.
[6] Nalwa HS, editor. Ferroelectric polymers. New York: Marcel Dekker; 1995.
[7] Lu Y, Claude J, Neese B, Zhang QM, Wang Q. J Am Chem Soc 2006; 128:8120.
[8] Chu B, Zhou X, Ren K, Lin M, Wang Q, Bauer F, et al. Science 2006;313:334.
[9] Rabuffi M, Picci G. IEEE Trans Plasma Sci 2002;30:1939.
[10] Furukawa T, Date M, Johnson GE. J Appl Phys 1983;54:1540.
[11] He X, Yao K, Gan BK. J Appl Phys 2005;97:084101.
[12] Furukawa T, Nakajima T, Takahashi Y. IEEE Trans Dielect Elect Insul 2006;13: 1120.
[13] Guan F, Wang J, Yang L, Guan B, Han K, Wang Q, et al. Adv Funct Mater 2011; 21:3176.
[14] Guan F, Wang J, Yang L, Tseng JK, Han K, Wang Q, et al. Macromolecules 2011; 44:2190.
[15] Guan F, Pan J, Wang J, Wang Q, Zhu L. Macromolecules 2010;43:384.
[16] Ranjan V, Yu L, Nardelli MB, Bernholc J. Phys Rev Lett 2007;99:047801.
[17] Claude J, Lu Y, Li K, Wang Q. Chem Mater 2008;20:2078.
[18] Yang X, Li Z, Odum L, Cheng ZY. Mater Res Soc Symp Proc 2006;889. W07.03.1.
[19] Duiker HM, Beale PD. Phys Rev B 1990;41:490.
[20] Furukawa T. Phase Trans 1989;18:143.
[21] Scott JF. Adv Mater 2010;22:5315.